

Displacement memory and \mathcal{B} -memory in generalised Ellis-Bronnikov wormholes

Soumya Bhattacharya,^{1,2} and Suman Ghosh³

¹*Department of Astrophysics and High Energy Physics,
S.N. Bose National Center for Basic Sciences, Kolkata 700106, India*

²*Inter-University Centre for Astronomy and Astrophysics (IUCAA),
Post Bag 4, Ganeshkhind, Pune, 411 007, India**

³*Department of Physics, Birla Institute of Technology, Mesra, Ranchi-835215, India[†]*

Gravitational wave (GW) memory effect is studied in the context of generalised Ellis-Bronnikov (GEB) wormholes. We solved the geodesic equations in this wormhole spacetime, in the presence of a GW pulse. The resulting evolution of the geodesic separation shows the presence of displacement and velocity memory. Memory effect due to a gravitational wave ensures that there is a permanent effect on spacetime geometry. The corresponding geodesic evolution, being metric dependent, would display distinct results in each case. Motivated by the same, we study further aspects of memory effect on the geodesic congruences, known as the \mathcal{B} -memory, by solving the Raychaudhuri equations. Since future GW detectors will be able to probe the memory effect, our work presents GEB spacetime as a black hole mimicker with distinguishing features.

I. INTRODUCTION

The direct detection of gravitational waves (GWs) from binary black holes and binary neutron star merger events [1, 2], as well as the observations of the shadow of supermassive compact central objects, e.g., the M87* and the SgrA* [3–7], are the two major observational breakthroughs in the field of gravitational physics within the last decade. Both of these observations depend crucially on the strong field behavior of gravity and, in principle, can be used to test the robustness of general relativity (GR) and also provide pointers to the nature of the compact objects. Despite the fact that—so far GR has passed these strong field tests without any scar—from a purely theoretical perspective, the inability of GR to correctly reconcile singularities occurring at the end point of gravitational collapse, or, as the starting point of our modern hot big-bang cosmology, poses a serious challenge to the theory itself. This important shortcoming of GR must make room for investigating alternative possibilities, *vis-à-vis* modified near-horizon geometries. Among the alternatives, one can look for non-black hole compact objects that can arise from quantum gravity-motivated theories, e.g., fuzzballs [8] or compact objects made out of exotic matter fields, known as exotic compact objects or ECOs [9–12].

An important question is whether it is possible to distinguish these so-called black hole mimickers from each other by studying GWs propagating in such background of ECOs. Wormholes [13, 14] are one such class of black hole mimickers that has its origin in general relativity (GR) itself. Although wormholes are speculative objects till date, recent studies of events such as wormhole merger

[15, 16] and their quasinormal modes [17, 18] can illuminate the detection prospects of wormholes in our universe. Here we are interested about another of such quite *unexplored* detection prospect, the GW memory effect.

One of the most studied traversable wormhole geometry is the four-dimensional Ellis-Bronnikov (EB) spacetime [19, 20], which is sustained by a phantom scalar field (a field with a negative kinetic term). The presence of negative energy density makes them difficult to realise in macroscopic quantities [21]. However, recently, it has been shown that, EB wormhole does partially satisfy energy condition in modified gravity theories such as through embedding in higher dimension [22], [23]. Further, violation of energy conditions can be avoided at the throat within GR by a simple modification leading to the so-called generalised Ellis-Bronnikov (GEB) model [24]. There have been a lot of works in different directions where this EB wormhole spacetime plays a central role, for example the role of phantom scalar field with non-linear electrodynamics in this context is studied in [25], gravitational lensing and deflection angle in [26], quasinormal modes in [27, 28], and in the context of various modified gravity theories [23, 29, 30].

In this article, we investigate a specific property of gravitational waves: the *memory effect* in GEB background [24]. The GW memory effect refers to the lasting change in the relative distance between test particles when a GW passes through the ambient spacetime [31, 32]. This effect encompasses both the strong-field, as well as non-linear aspects of general relativity, which is yet to be observed. It is already proposed to be detected in advanced LIGO and VIRGO [33] and in LISA [34]. In recent times, there has been a lot of works on various theoretical aspects of memory effect [35–42]. In [43, 44], it is shown how the signature of the wormhole “hairs” gets imprinted on the memory signal. Recently, it has been emphasized that, in addition to the usual displacement and velocity memory effect, geodesic congruences also experience such

* soumya557@gmail.com

† suman.ghosh@bitmesra.ac.in

an effect known as the \mathcal{B} -memory [45]. We discuss about this approach later in more detail. Our main motivation here is to investigate how the memory effect depends on the ambient GEB spacetime. This can be understood specifically by studying the dependence of the memory effect on the wormhole parameters or the so-called *wormhole hairs*.

In Section II, we briefly introduce the GEB wormhole model. In Section III, we computed both displacement and velocity memory effects in a background GEB spacetime and then compared them with the memory effect in the Schwarzschild background. We particularly highlight the differences in memory effect when the background evolution is eliminated. In Section IV, we use the Raychaudhuri equation to show that memory effect is visible in the evolution of the geodesic congruences as well. We summarise our results with a brief discussion on future avenues in Section V.

II. GEB WORMHOLE GEOMETRY

The GEB wormhole line element [24] is described in Schwarzschild-like coordinates as,

$$ds^2 = -dt^2 + \frac{dr^2}{1 - \frac{b(r)}{r}} + r^2 d\Omega_2^2, \quad (1)$$

where $d\Omega_2^2 = d\theta^2 + \sin^2\theta d\phi^2$ is the solid angle and the shape function $b(r)$ is given by

$$b(r) = r - r^{(3-2m)}(r^m - b_0^m)^{(2-\frac{2}{m})}. \quad (2)$$

One gets back the EB geometry, for $m = 2$, which is a static, spherically symmetric, geodesically complete, horizonless space-time (constructed using phantom scalar field). Considering the Morris–Thorne conditions [46] as necessary conditions to construct a Lorentzian wormhole, Kar et al. [24] introduced the GEB model as a two-parameter (m and b_0) family of Lorentzian wormholes. Here, b_0 is the so-called ‘throat radius’ of the wormhole and m is the wormhole ‘steepness’ parameter that can take only even values ($m \geq 2$, to ensure the smoothness of the function $r(l)$). Let us introduce a tortoise coordinate l such that

$$dl = \frac{dr}{\sqrt{\left(1 - \frac{b(r)}{r}\right)}}. \quad (3)$$

In this coordinate the line element looks like

$$ds^2 = -dt^2 + dl^2 + r(l)^2 \left(d\theta^2 + \sin^2\theta d\phi^2 \right), \quad (4)$$

where

$$r(l) = (b_0^m + l^m)^{\frac{1}{m}}. \quad (5)$$

One can see that $l \rightarrow \pm\infty$ are the flat asymptotics. While solving for the memory effect we shall express the line element given in Eq. (4) in Bondi-Sachs form as,

$$ds^2 = -du^2 - 2dudl + r^2(l) d\Omega_2^2, \quad (6)$$

where $u = t - l$ is the outgoing light-cone coordinate. We are going to study the evolution of the geodesics in the wormhole background, presented above, in presence of a GW pulse and study how the displacement and velocity memory effects depend on the wormhole nature of the background geometry. For this purpose, we write down the spacetime metric as a sum of the background wormhole geometry $g_{\mu\nu}$ and a GW perturbation $h_{\mu\nu}$, such that the line element becomes,

$$ds^2 = (g_{\mu\nu} + h_{\mu\nu})dx^\mu dx^\nu \quad (7)$$

Using the wormhole geometry presented in Eq. (6), the resulting geometry becomes,

$$ds^2 = -du^2 - 2dudl + [r^2(l) + r(l) H(u)]d\theta^2 + [r^2(l) - r(l) H(u)]\sin^2\theta d\phi^2 \quad (8)$$

Here $H(u)$ is the GW perturbation and we can assume that it can be expressed in transverse-traceless (TT) gauge. In the following section, we present the analysis of the GW memory effect for GEB wormhole geometry, along with the case of Schwarzschild geometry as well.

III. MEMORY EFFECT THROUGH GEODESIC ANALYSIS

In this section, we will present the analysis of the memory effect vis-a-vis the geodesic deviation between neighbouring geodesics due to a propagating GW, with the geodesic separation quantifying the amount of displacement memory effect. Moreover, if the geodesics do not have constant separation, after the passage of the GW pulse, one can also associate a velocity memory effect with these geodesics as well. Before going in to the wormhole scenario we will briefly discuss the Schwarzschild case here.

A. Memory effect in GEB background

We can write down the geodesic equations for the line element given in Eq. (8) for u , l , θ and ϕ coordinates as

$$\ddot{u} + \frac{r'}{2} (2r + H) \dot{\theta}^2 + \frac{r'}{2} (2r - H) \sin^2\theta \dot{\phi}^2 = 0. \quad (9)$$

$$\ddot{l} - \frac{1}{2} (2rr' + r'H - rH') \dot{\theta}^2 - \frac{1}{2} (2rr' - r'H + rH') \sin^2\theta \dot{\phi}^2 = 0. \quad (10)$$

$$\ddot{\theta} + \frac{H'}{H+r} \dot{u} \dot{\theta} + \frac{(2r+H)r'}{(r+H)r} \dot{l} \dot{\theta} - \frac{r-H}{r+H} \sin \theta \cos \theta \dot{\phi}^2 = 0. \quad (11)$$

$$\ddot{\phi} - \frac{H'}{r-H} \dot{u} \dot{\phi} + \frac{(2r-H)r'}{(r-H)r} \dot{l} \dot{\phi} + 2 \cot \theta \dot{\theta} \dot{\phi} = 0 \quad (12)$$

Here ‘overdot’ denotes derivative with respect to the proper time τ associated with the geodesics, while ‘prime’ denotes derivative with respect to the argument of the respective function. For example, $H'(u) \equiv (dH/du)$ and $r'(l) \equiv (dr/dl)$.

We have solved the three geodesic equations, presented in Eq. (9) - Eq. (12), numerically using the standard software package *MATHEMATICA* and have analysed the solutions graphically. In particular, we have started by considering two neighbouring geodesics in the wormhole background and then studied the evolution of their coordinate separation. To study the memory effect, we confine ourself in the equatorial ($\theta = \pi/2$) plane and analyse the evolution of geodesic separation along l & ϕ coordinates. Schematically we can represent them as

$$\begin{aligned} \Delta l &\equiv l(\text{Geodesic II}) - l(\text{Geodesic I}), \\ \Delta \phi &\equiv \phi(\text{Geodesic II}) - \phi(\text{Geodesic I}). \end{aligned}$$

We determine the evolution of the quantities Δl & $\Delta \phi$ both in presence and absence of GW pulse.

Since we are considering time-like geodesics, they will satisfy following condition

$$\begin{aligned} -\dot{u}^2 - 2 \dot{u} \dot{l} + [r^2(l) + r(l) H(u)] \dot{\theta}^2 \\ + [r^2(l) - r(l) H(u)] \sin^2 \theta \dot{\phi}^2 = -1. \end{aligned} \quad (13)$$

Now, for our case, we take the gravitational wave pulse profile as

$$H(u) = A \operatorname{sech}^2(u - u_0). \quad (14)$$

Note that positive definiteness of the metric compo-

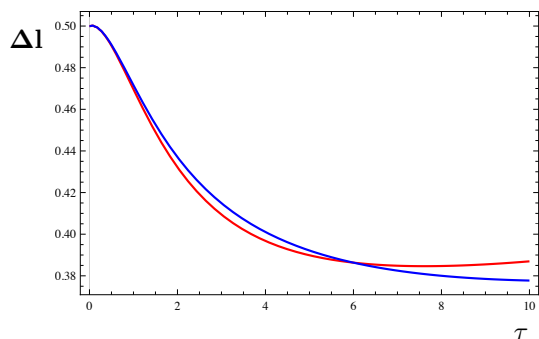


FIG. 1. Plot of the evolution of the l geodesic in presence (red curve) and absence (blue curve) of GW for $m = 2$ (EB) model.

nent $g_{\phi\phi}$ implies $r > H$ which for our choice of models implies $b_0 > A$. In the following, for numerical evalua-

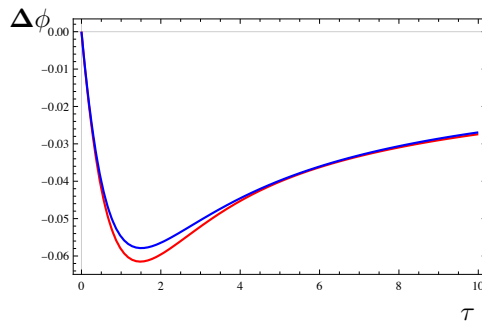


FIG. 2. Plot of the evolution of the ϕ geodesic in presence (red curve) and absence (blue curve) of GW for $m = 2$ model.

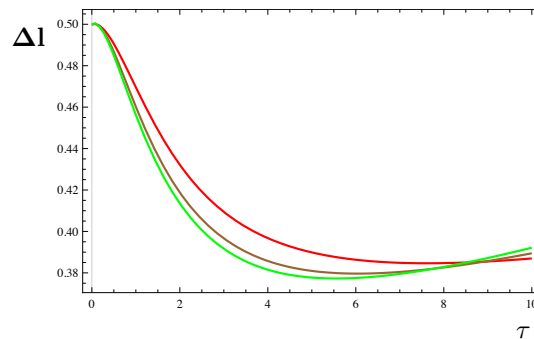


FIG. 3. Plot of the evolution of the l geodesic in the presence of GW for $m = 2$ (red), $m = 4$ (brown) and $m = 6$ (green) model.

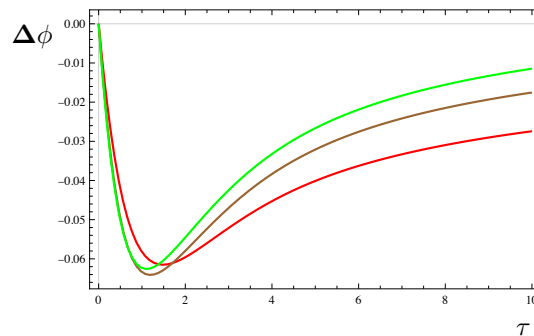


FIG. 4. Plot of the evolution of the ϕ geodesic in presence of GW for $m = 2$ (red), $m = 4$ (brown) and $m = 6$ (green) model.

tion, we chose a fixed value of $A = 1/2$ and we choice of $b_0 > 1/2$. Figures 1-2 depict the displacement memory effect along l and ϕ directions respectively. It is clear that effect on Δl is considerably large compared to $\Delta \phi$. Figures 5-6 show that decreasing the throat radius b_0 , while keeping the steepness parameter m fixed, leads to a scenario similar to increasing m while keeping b_0 fixed as shown in figures 3-4. This happens because for both choices the gravitational pulse effectively passes through a region with lower curvature in the wormhole spacetime. In figures 7-8 we have shown the displacement memory effect by subtracting background evolution. In Fig. 9 the

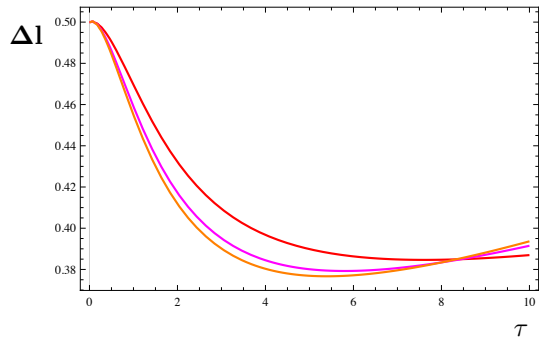


FIG. 5. Plot of the evolution of the l geodesic in presence of GW for $b_0 = 1.0$ (red), $b_0 = 0.5$ (magenta) and $b_0 = 0.1$ (orange) in $m = 2$ model.

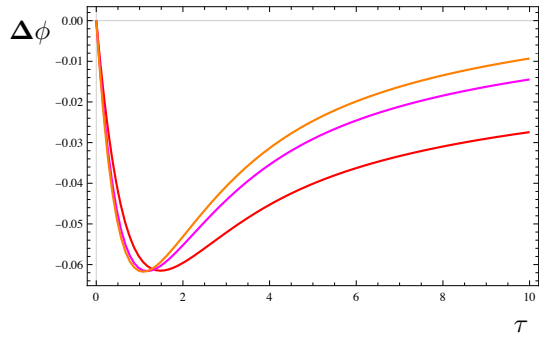


FIG. 6. Plot of the evolution of the ϕ geodesic in presence of GW for $b_0 = 1.0$ (red), $b_0 = 0.5$ (magenta) and $b_0 = 0.1$ (orange) in $m = 2$ model.

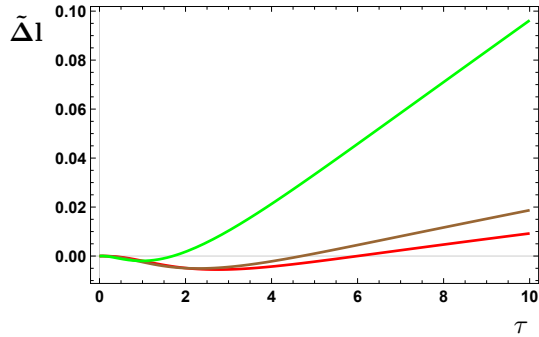


FIG. 7. Plot of the evolution of the l geodesic only in the presence of GW (subtracting the background evolution) for $m = 2$ (red), $m = 4$ (brown) and $m = 6$ (green) model.

evolution of Δl is considered with respect to l for two different values of m ($m = 6$ (green) and $m = 4$ (brown)) both in presence (solid line) and absence (dotted line) of the GW pulse. One can clearly see the difference between the dotted line and solid line depends on the wormhole parameter m , which indicates the fact that as m increases so is the displacement memory effect. We can see the similar characteristics from figures 7-8 as well.

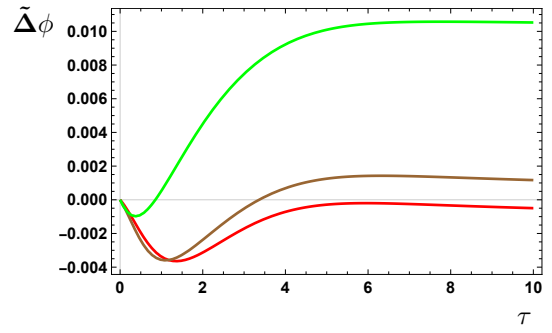


FIG. 8. Plot of the evolution of the ϕ geodesic only in presence of GW (subtracting the background evolution) for $m = 2$ (red), $m = 4$ (brown) and $m = 6$ (green) model.

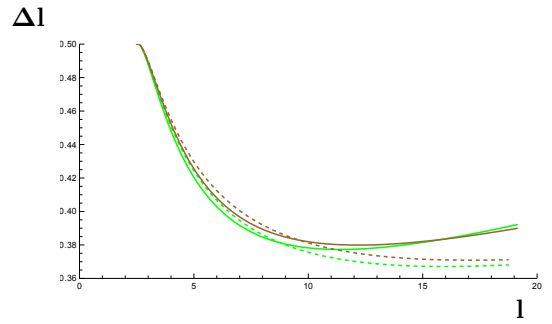


FIG. 9. Plot of the evolution of the separation along l geodesics, Δl , with respect to r , in presence (solid line), and absence (dotted line) of GW pulse for $m = 6$ (green) and $m = 4$ (brown).

B. Memory effect in Schwarzschild background

We choose the outgoing Eddington-Finkelstein coordinate system (which makes use of the tortoise coordinate r_*) for convenience and the corresponding line element looks as follows,

$$ds^2 = -f(r) du^2 - 2 du dr + r^2 d\theta^2 + r^2 \sin^2 \theta d\phi^2. \quad (15)$$

Where $f(r) = (1 - \frac{2m}{r})$. Due to the presence of a GW perturbation $h_{\mu\nu}$, resulting line element becomes,

$$ds^2 = (g_{\mu\nu} + h_{\mu\nu}) dx^\mu dx^\nu. \quad (16)$$

If we consider the cross-components of the GW to be zero for simplicity then we can write the line element in Eq. (16) in transverse-traceless (TT) gauge as follows

$$ds^2 = -f(r) du^2 - 2 du dr + (r^2 + rH(u)) d\theta^2 + (r^2 - rH(u)) \sin^2 \theta d\phi^2. \quad (17)$$

Corresponding to this, the geodesic equations in the equatorial ($\theta = \pi/2$) plane would be

$$\ddot{u} - \frac{f'(r)}{2} \dot{u}^2 + \frac{(2r - H(u))}{2} \dot{\phi}^2 = 0 \quad (18)$$

$$\ddot{r} + \frac{f'(r)f(r)}{2} \dot{u}^2 - \frac{(2r + H(u))f(r)}{2} \dot{\phi}^2 + f'(r) \dot{u} \dot{r} - \frac{r H'(u)}{2} \dot{\phi}^2 = 0 \quad (19)$$

$$\ddot{\phi} + \left(\frac{2r\dot{r} - H(u)\dot{r} - rH'(u)\dot{u}}{r^2 - rH(u)} \right) \dot{\phi} = 0 \quad (20)$$

The displacement memory effect along the radial and

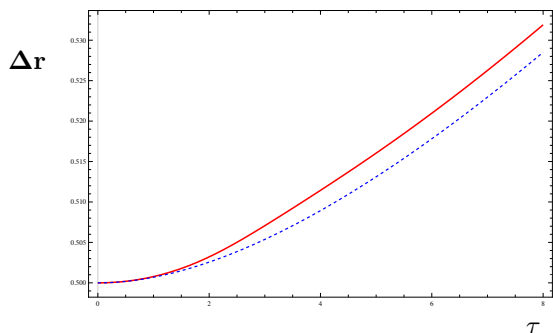


FIG. 10. Plot of the evolution of the r geodesic in presence (red) and absence (blue dotted) of GW.

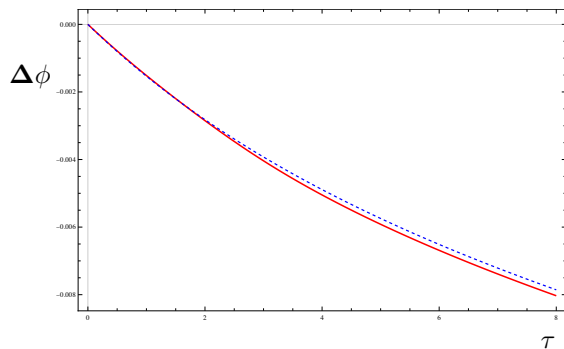


FIG. 11. Plot of the evolution of the ϕ geodesic in presence (red) and absence (blue dotted) of GW.

polar direction have been depicted in figures 10 and 11 respectively. Here we can see that evolution of Δr and $\Delta\phi$ (vs τ) overlaps initially, but after the passage of gravitational wave pulse they evolve differently. Also the non-constant separation between them is the indication of the presence of a *velocity memory* effect. In Fig. 12 we have shown the evolution of Δr with respect to r that agrees with Fig. 10 and clearly shows how the memory effect saturates.

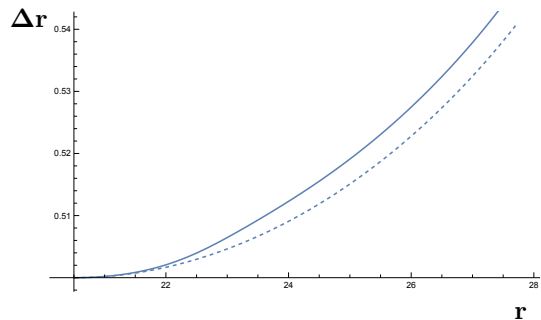


FIG. 12. Plot of the evolution of the separation along r geodesics, Δr , with respect to r , in presence (solid line), and absence (dotted line) of GW pulse.

IV. \mathcal{B} -MEMORY IN GEB SPACETIME

Solving geodesic equations and geodesic deviation equation leads to possible displacement memory effect in general. However, geodesic equation can reveal velocity memory as well. The memory effect involving geodesic congruence is closer to the velocity memory but not quite the same. A covariant approach of looking at the behavior of geodesic congruences has been proposed recently by O’Loughlin and Demirchian [47], wherein the term \mathcal{B} -memory (\mathcal{B} denotes the covariant gradient of the velocity field) is introduced in the context of impulsive gravitational waves. This approach naturally implies that one can solve Raychaudhuri equation to reveal memory effect on kinematic properties of a congruence. In [48], Raychaudhuri equation is used to study the memory effect on a congruence of geodesics, in exact plane wave spacetimes expressed in the Brinkmann coordinates. They found that for a growth (or decay) of shear causes focusing of an initially parallel congruence, after the departure of the pulse. Remarkably, a correlation between the “focusing time” (the affine parameter) and the amplitude and phase of the pulse (or its derivatives) is found. Such features distinctly suggest presence of the so-called \mathcal{B} -memory. In the following, by solving the Raychaudhuri equation, we reveal qualitative features of the memory effect in the evolution of a geodesic congruence in GEB spacetimes (for various choices of the wormhole parameters), when a gravitational pulse passes through it.

One may derive the ESR variables directly from the following definitions [49–53] for the expansion scalar Θ , the shear tensor $\Sigma_{\alpha\beta}$ and the rotation tensor $\Omega_{\alpha\beta}$, by first solving for the geodesic vector field u^α ,

$$\Theta = \nabla_\alpha u^\alpha, \quad (21)$$

$$\Sigma_{\alpha\beta} = \frac{1}{2} (\nabla_\beta u_\alpha + \nabla_\alpha u_\beta) - \frac{1}{n-1} h_{\alpha\beta} \Theta, \quad (22)$$

$$\Omega_{\alpha\beta} = \frac{1}{2} (\nabla_\beta u_\alpha - \nabla_\alpha u_\beta). \quad (23)$$

Here, n is the dimension of spacetime and $h_{\alpha\beta} = g_{\alpha\beta} \pm u_\alpha u_\beta$ is the projection tensor (the plus sign is for timelike

curves whereas the minus one is for spacelike ones) and $u_\alpha u^\alpha = \mp 1$.

One can also first solve the following equation [49]

$$u^\mu \nabla_\mu \mathcal{B}_{\alpha\beta} = -\mathcal{B}_{\alpha\mu} \mathcal{B}^\mu{}_\beta - R_{\alpha\mu\beta\nu} u^\mu u^\nu, \quad (24)$$

where the \mathcal{B} -tensor is given by,

$$\mathcal{B}_{\alpha\beta} = \nabla_\beta u_\alpha = \frac{1}{n-1} \theta h_{\alpha\beta} + \sigma_{\alpha\beta} + \omega_{\alpha\beta}, \quad (25)$$

along with the geodesic equations. Then it is easy to determine the so-called ESR variables from $\mathcal{B}_{\alpha\beta}$ using the definitions in Eqs. (21 - 23). One can separate Eq. (24), into the following three equations for trace, antisymmetric and symmetric traceless parts of $\mathcal{B}_{\alpha\beta}$ as,

$$\frac{d\Theta}{d\lambda} + \frac{1}{n-1} \Theta^2 + \sigma^2 - \omega^2 = -R_{\alpha\beta} u^\alpha u^\beta, \quad (26)$$

$$\frac{d\sigma_{\alpha\beta}}{d\lambda} = -\frac{2}{n-1} \Theta \sigma_{\alpha\beta} - \sigma_{\alpha\gamma} \sigma^\gamma{}_\beta + \omega_{\alpha\gamma} \omega^\gamma{}_\beta - \frac{1}{n-1} h_{\alpha\beta} (\sigma^2 - \omega^2) + C_{\mu\beta\alpha\nu} u^\mu u^\nu + \frac{1}{n-1} \tilde{R}_{\alpha\beta}, \quad (27)$$

$$\frac{d\omega_{\alpha\beta}}{d\lambda} = -\frac{2}{n-1} \Theta \omega_{\alpha\beta} - \sigma^\gamma{}_\beta \omega_{\alpha\gamma} + \sigma^\gamma{}_\alpha \omega_{\beta\gamma}, \quad (28)$$

where, $\sigma^2 = \sigma_{\alpha\beta} \sigma^{\alpha\beta}$, $\omega^2 = \omega_{\alpha\beta} \omega^{\alpha\beta}$ and $C_{\mu\beta\alpha\nu}$ is the Weyl tensor and $\tilde{R}_{\alpha\beta} = h_{\alpha\mu} h_{\nu\beta} R^{\mu\nu} - \frac{1}{n-1} h_{\alpha\beta} h_{\mu\nu} R^{\mu\nu}$. Note that, these are not equations but, identities. In some scenarios [54–56], however, we find that the identities become equations once we use the Einstein equations or any other geometric property (e.g. Einstein space, or vacuum, etc.) as an input. To see the evolution from a local observer's viewpoint [57], one can solve the geodesic deviation equation too and express the tensorial quantities in the frame basis. The metric tensor in the coordinate basis and frame basis are related as

$$g^{\alpha\beta} = e^\alpha{}_a e^\beta{}_b \eta^{ab}, \quad (29)$$

where the vierbein field, $e^\alpha{}_a$, has two indices, ‘ α ’ labels the general spacetime coordinate (the coordinate basis) and ‘ a ’ labels the local Lorentz spacetime or local laboratory coordinates (the frame basis). However, we do not present the evolution with respect to the local observer in this article and only look at the evolution of ESR variables by numerically solving Eq. (24).

We present, in Fig. 13, the evolution of the expansion scalar and the shear amplitude for congruence of timelike geodesics that are crossing the EB wormhole ($m = 2$) passage from positive to negative l . Here we assume a non-rotating congruence for simplicity. Boundary conditions are set such that $\mathcal{B}_{\alpha\beta}(l = 0) = 0$ i.e., disappearing expansion and shear when the congruence crosses the wormhole throat (i.e. $l = 0$ at $\tau = 0$). For the ‘central’ geodesic, boundary conditions are chosen

such that U and l coordinates evolve linearly with the affine parameter and θ and ϕ coordinates remain constant ($\dot{u}(0) = \sqrt{2} - 1, \dot{l}(0) = 1, \dot{\theta}(0) = \dot{\phi}(0) = 0$ and $u(0) = 0, l(0) = 0, \theta(0) = \pi/2, \phi(0) = 0$). Thus, the central geodesic, which is a radial geodesic, does not see any effect of the gravitational pulse as such, which is clear from the geodesic equations. Note that it is the curvature term in Eq. (24) that determines the evolution of the congruence. In the figures, the continuous and dotted lines represent congruences in absence and presence of the gravitational pulse, respectively. The initial conditions for the pulse are chosen so that the pulse reaches the throat at the same time that the congruence arrives. For all numerical estimations, we have chosen $b_0 = 1$ like in the previous section. Note that the results in the absence of the pulse matches with the results reported earlier [58, 59] (where the non-null coordinates were used), thus assuring accuracy of our numerical evaluation.

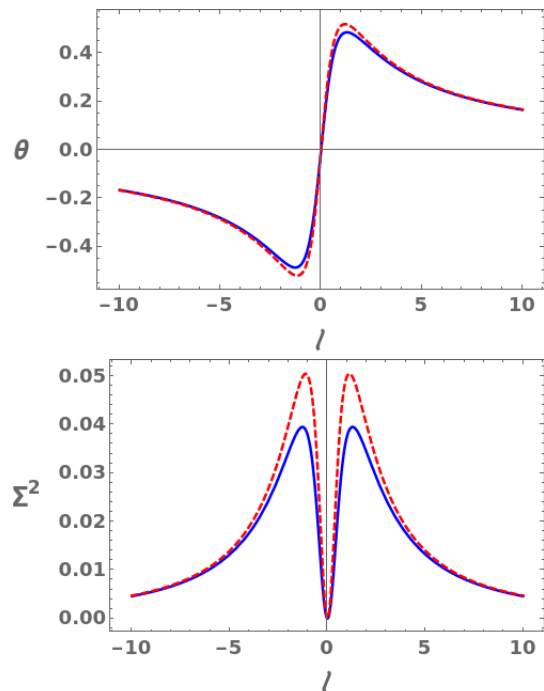


FIG. 13. Expansion scalar and the shear amplitude for congruence of timelike geodesics for $m = 2$ model.

Fig. 13 shows that on a background EB spacetime (i.e. $m = 2$), the pulse results in increased total expansion and shear deformation of the congruence. Fig. 14 and Fig. 15 show similar features for $m = 4$ and $m = 6$ geometries, however the amount of increase in deformation decreases slightly with increasing m . As a clearer signature of higher- m geometry (irrespective of pulse-effect), we see that the passage through the throat becomes more and more *stable* for higher m or wormholes with steeper neck. The presence of the pulse could not alter the ESR Profiles at the ‘zero-deformation’ region where the congruence crosses the throat. We observe that the location where the effect of the pulse is maximum, approaches $l = b_0$ as

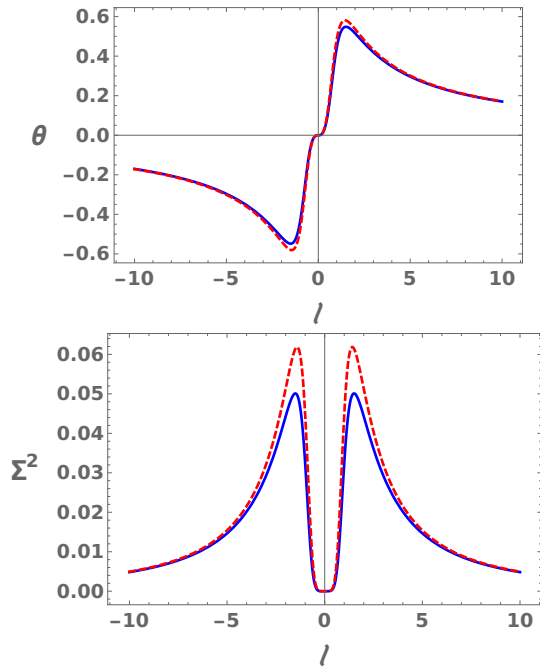


FIG. 14. Expansion scalar and the shear amplitude for congruence of timelike geodesics for $m = 4$ model.

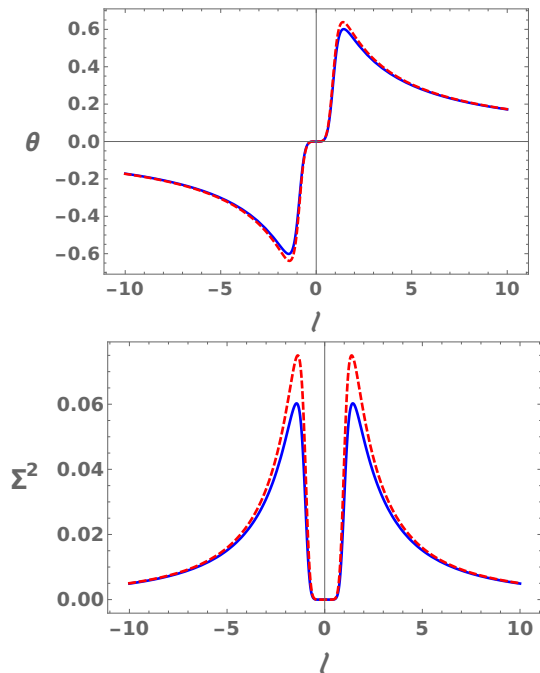


FIG. 15. Expansion scalar and the shear amplitude for congruence of timelike geodesics for $m = 6$ model.

we increase the value of m .

Fig. 16, show the evolutions of expansion and shear in presence of a pulse with varying throat radius. These patterns can be understood as follows. As we lower the length scale of the wormhole compared to the length scale

of the pulse (which is fixed) the pulse becomes more and more dominant factor in determining the kinematic evolution of the geodesic congruence thus imparting a larger \mathcal{B} -memory effect.

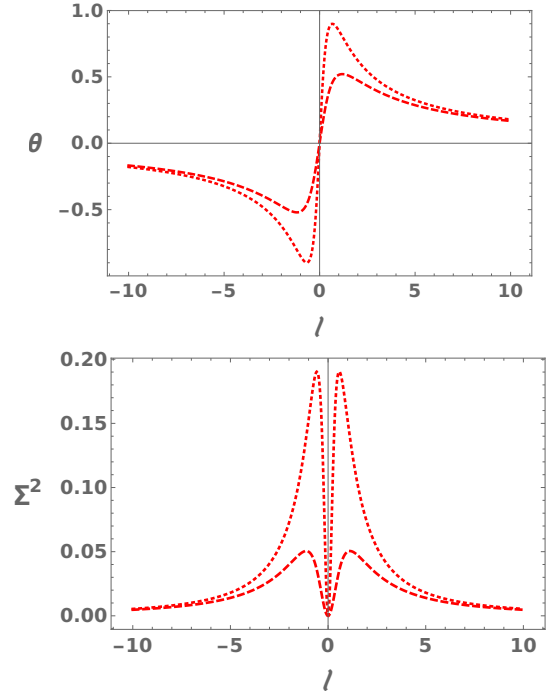


FIG. 16. The dashed curve correspond to $b = 1$ and the dotted curves correspond to $b = 2/3$.

V. DISCUSSIONS

With the current advancements in gravitational wave research and the promise of highly sensitive upcoming detectors, we now have the opportunity of studying systems and phenomena which were out of our reach before. Memory effect is one such event whose detection is becoming more realistic with the improving technology of gravitational wave detectors. Let us summarize, point by point, the significant aspects and findings of the paper.

- In this article, we have explored certain features of the GW memory in the generalised Ellis-Bronnikov wormhole spacetime. Being the oldest candidate of the class of ECOs, wormholes have always been an interesting subject of research from astrophysical point of view. We, at first, have briefly reviewed the geometry of the wormhole spacetime. Then we have explored the displacement memory effects by analyzing neighboring geodesics and the geodesic congruences in the wormhole background in presence of a localized GW pulse.
- We have shown explicitly, how the geodesic separation evolves before and after the passage of the

pulse. This explicitly establishes the existence of displacement memory effect. The non-linear evolution of the separation of the geodesics is a clear manifestation of *velocity memory*. Also we have shown through various plots how the memory effect depends on the wormhole *hairs*, b_0 and m , and thus validates our claim that memory effect is indeed a future pointer towards exploring the existence of non-blackhole compact objects in our universe.

- Motivated by these results, we study further aspects of memory effect on the geodesic congruences using the Raychaudhuri equations– the so-called \mathcal{B} -memory effect. The memory effect involving geodesic congruence does not exactly mimics velocity memory in general. Evolution of expansion and shear shows an increase of total deformation of the congruence in presence of the pulse.
- As expected, we found that \mathcal{B} -memory effects also depend crucially on the *hairs* or the wormhole parameters. For example, for higher m -geometries the \mathcal{B} -memory effect gets smaller. Hence it is expected to differ from the corresponding memory effects for different wormholes or other compact objects. We believe this observation can safely lead us to the claim that memory effects are indeed future pointers toward exploring the existence of non-black hole

compact objects in our universe.

Although we have considered static and spherically symmetric wormhole solution here, observational data indicates that most astrophysical systems in our universe undergo rotation. Hence a possible future goal would be to study gravitational memory effect in the case of rotating wormholes [60] (which presents new challenges). See also a recent work [61], where a method was proposed to generate rotating Lorentzian wormholes. It would be interesting to see how the memory effect, for example, in a rotating wormhole would differ from a stationary wormhole as well as black holes. On another front, GW memory effect can be studied using symmetries at null infinity using the Bondi-Sachs formalism to explore how the Bondi mass varies, as formulated in [43]. We shall address these issues and more elsewhere.

ACKNOWLEDGEMENTS

Authors would like to thank Sayan Kar and Sumanta Chakraborty for discussions and suggestions. SB would like to acknowledge IUCAA Pune for providing necessary facilities under the visitor’s programme. SG acknowledges grant provided by BIT Mesra (DRIE/SMS/DRIE-05/2023-24/2352).

-
- [1] **LIGO Scientific, Virgo** Collaboration, B. P. Abbott *et al.*, “Observation of Gravitational Waves from a Binary Black Hole Merger,” *Phys. Rev. Lett.* **116** no. 6, (2016) 061102, [arXiv:1602.03837 \[gr-qc\]](#).
- [2] **LIGO Scientific, Virgo** Collaboration, B. P. Abbott *et al.*, “GW170817: Observation of Gravitational Waves from a Binary Neutron Star Inspiral,” *Phys. Rev. Lett.* **119** no. 16, (2017) 161101, [arXiv:1710.05832 \[gr-qc\]](#).
- [3] **Event Horizon Telescope** Collaboration, K. Akiyama *et al.*, “First M87 Event Horizon Telescope Results. I. The Shadow of the Supermassive Black Hole,” *Astrophys. J. Lett.* **875** (2019) L1, [arXiv:1906.11238 \[astro-ph.GA\]](#).
- [4] **Event Horizon Telescope** Collaboration, K. Akiyama *et al.*, “First M87 Event Horizon Telescope Results. II. Array and Instrumentation,” *Astrophys. J. Lett.* **875** no. 1, (2019) L2, [arXiv:1906.11239 \[astro-ph.IM\]](#).
- [5] **Event Horizon Telescope** Collaboration, K. Akiyama *et al.*, “First M87 Event Horizon Telescope Results. III. Data Processing and Calibration,” *Astrophys. J. Lett.* **875** no. 1, (2019) L3, [arXiv:1906.11240 \[astro-ph.GA\]](#).
- [6] **Event Horizon Telescope** Collaboration, K. Akiyama *et al.*, “First M87 Event Horizon Telescope Results. IV. Imaging the Central Supermassive Black Hole,” *Astrophys. J. Lett.* **875** no. 1, (2019) L4, [arXiv:1906.11241 \[astro-ph.GA\]](#).
- [7] **Event Horizon Telescope** Collaboration, K. Akiyama *et al.*, “First M87 Event Horizon Telescope Results. V. Physical Origin of the Asymmetric Ring,” *Astrophys. J. Lett.* **875** no. 1, (2019) L5, [arXiv:1906.11242 \[astro-ph.GA\]](#).
- [8] S. D. Mathur, “The Fuzzball proposal for black holes: An Elementary review,” *Fortsch. Phys.* **53** (2005) 793–827, [arXiv:hep-th/0502050](#).
- [9] V. Cardoso and P. Pani, “Testing the nature of dark compact objects: a status report,” *Living Rev. Rel.* **22** no. 1, (2019) 4, [arXiv:1904.05363 \[gr-qc\]](#).
- [10] Z. Mark, A. Zimmerman, S. M. Du, and Y. Chen, “A recipe for echoes from exotic compact objects,” *Phys. Rev. D* **96** no. 8, (2017) 084002, [arXiv:1706.06155 \[gr-qc\]](#).
- [11] V. Cardoso, S. Hopper, C. F. B. Macedo, C. Palenzuela, and P. Pani, “Gravitational-wave signatures of exotic compact objects and of quantum corrections at the horizon scale,” *Phys. Rev. D* **94** no. 8, (2016) 084031, [arXiv:1608.08637 \[gr-qc\]](#).
- [12] S. Murk, “Nomen non est omen: Why it is too soon to identify ultra-compact objects as black holes,” *Int. J. Mod. Phys. D* **32** (2023) 2342012, [arXiv:2210.03750 \[gr-qc\]](#).
- [13] M. S. Morris, K. S. Thorne, and U. Yurtsever, “Wormholes, time machines, and the weak energy condition,” *Phys. Rev. Lett.* **61** (Sep, 1988) 1446–1449. <https://link.aps.org/doi/10.1103/PhysRevLett.61.1446>.
- [14] K. A. Bronnikov, V. N. Melnikov, and H. Dehnen, “General class of brane-world black holes,” *Phys. Rev. D* **68** (Jul, 2003) 024025. <https://link.aps.org/doi/10.1103/PhysRevD.68.024025>.

- [15] N. V. Krishnendu, K. G. Arun, and C. K. Mishra, “Testing the binary black hole nature of a compact binary coalescence,” *Phys. Rev. Lett.* **119** no. 9, (2017) 091101, [arXiv:1701.06318](https://arxiv.org/abs/1701.06318) [gr-qc].
- [16] V. Cardoso, E. Franzin, and P. Pani, “Is the gravitational-wave ringdown a probe of the event horizon?,” *Phys. Rev. Lett.* **116** (Apr, 2016) 171101. <https://link.aps.org/doi/10.1103/PhysRevLett.116.171101>.
- [17] S. Aneesh, S. Bose, and S. Kar, “Gravitational waves from quasinormal modes of a class of lorentzian wormholes,” *Phys. Rev. D* **97** (Jun, 2018) 124004. <https://link.aps.org/doi/10.1103/PhysRevD.97.124004>.
- [18] P. Dutta Roy, S. Aneesh, and S. Kar, “Revisiting a family of wormholes: geometry, matter, scalar quasinormal modes and echoes,” *Eur. Phys. J. C* **80** no. 9, (2020) 850, [arXiv:1910.08746](https://arxiv.org/abs/1910.08746) [gr-qc].
- [19] H. G. Ellis, “Ether flow through a drainhole: A particle model in general relativity,” *Journal of Mathematical Physics* **14** no. 1, (1973) 104–118, <https://doi.org/10.1063/1.1666161>. <https://doi.org/10.1063/1.1666161>.
- [20] K. A. Bronnikov, “Scalar-tensor theory and scalar charge,” *Acta Phys. Polon. B* **4** (1973) 251–266.
- [21] E. Witten, “Light Rays, Singularities, and All That,” *Rev. Mod. Phys.* **92** no. 4, (2020) 045004, [arXiv:1901.03928](https://arxiv.org/abs/1901.03928) [hep-th].
- [22] S. Kar, S. Lahiri, and S. SenGupta, “Can extra dimensional effects allow wormholes without exotic matter?,” *Phys. Lett. B* **750** (2015) 319–324, [arXiv:1505.06831](https://arxiv.org/abs/1505.06831) [gr-qc].
- [23] V. Sharma and S. Ghosh, “Generalised Ellis–Bronnikov wormholes embedded in warped braneworld background and energy conditions,” *Eur. Phys. J. C* **81** no. 11, (2021) 1004, [arXiv:2111.07329](https://arxiv.org/abs/2111.07329) [gr-qc].
- [24] S. Kar, S. Minwalla, D. Mishra, and D. Sahdev, “Resonances in the transmission of massless scalar waves in a class of wormholes,” *Phys. Rev. D* **51** (1995) 1632–1638.
- [25] T. M. Crispim, G. Alencar, and C. R. Muniz, “Field sources for generalized ellis-bronnikov wormhole,” 2024. <https://arxiv.org/abs/2410.11147>.
- [26] S. Jana, V. Sharma, and S. Ghosh, “Gravitational lensing and deflection angle by generalised ellis-bronnikov wormhole embedded in warped braneworld background,” 2024. <https://arxiv.org/abs/2411.10804>.
- [27] A. Mitra and S. Ghosh, “Signature quasinormal modes of ellis-bronnikov wormhole embedded in warped braneworld background,” *Phys. Rev. D* **109** (Mar, 2024) 064005. <https://link.aps.org/doi/10.1103/PhysRevD.109.064005>.
- [28] F. S. Khoo, B. Azad, J. L. Blázquez-Salcedo, L. M. González-Romero, B. Kleihaus, J. Kunz, and F. Navarro-Lérida, “Quasinormal modes of rapidly rotating ellis-bronnikov wormholes,” *Physical Review D* **109** no. 8, (Apr., 2024) . <https://dx.doi.org/10.1103/PhysRevD.109.084013>.
- [29] M. Nilton, J. Furtado, G. Alencar, and R. Landim, “Generalized ellis-bronnikov wormholes in asymptotically safe gravity,” *Annals of Physics* **448** (Jan., 2023) 169195. <https://dx.doi.org/10.1016/j.aop.2022.169195>.
- [30] O. Sokoliuk, S. Mandal, P. K. Sahoo, and A. Baransky, “Generalised ellis-bronnikov wormholes in $f(r)$ gravity,” *The European Physical Journal C* **82** no. 4, (Apr., 2022) . <https://dx.doi.org/10.1140/epjc/s10052-022-10249-5>.
- [31] V. B. Braginsky and L. P. Grishchuk, “Kinematic Resonance and Memory Effect in Free Mass Gravitational Antennas,” *Sov. Phys. JETP* **62** (1985) 427–430.
- [32] M. Favata, “The gravitational-wave memory effect,” *Class. Qtm. Grav.* **27** no. 8, (Apr, 2010) 084036.
- [33] O. M. Boersma, D. A. Nichols, and P. Schmidt, “Forecasts for detecting the gravitational-wave memory effect with advanced ligo and virgo,” *Phys. Rev. D* **101** (Apr, 2020) 083026. <https://link.aps.org/doi/10.1103/PhysRevD.101.083026>.
- [34] **LISA Consortium Waveform Working Group** Collaboration, N. Afshordi *et al.*, “Waveform Modelling for the Laser Interferometer Space Antenna,” [arXiv:2311.01300](https://arxiv.org/abs/2311.01300) [gr-qc].
- [35] P.-M. Zhang, C. Duval, G. Gibbons, and P. Horvathy, “The memory effect for plane gravitational waves,” *Physics Letters B* **772** (Sept., 2017) 743–746. <https://dx.doi.org/10.1016/j.physletb.2017.07.050>.
- [36] P.-M. Zhang, C. Duval, G. Gibbons, and P. Horvathy, “Soft gravitons and the memory effect for plane gravitational waves,” *Physical Review D* **96** no. 6, (Sept., 2017) . <https://dx.doi.org/10.1103/PhysRevD.96.064013>.
- [37] P.-M. Zhang, C. Duval, G. Gibbons, and P. Horvathy, “Velocity memory effect for polarized gravitational waves,” *Journal of Cosmology and Astroparticle Physics* **2018** no. 05, (May, 2018) 030–030. <https://dx.doi.org/10.1088/1475-7516/2018/05/030>.
- [38] S. Bhattacharjee, S. Kumar, and A. Bhattacharyya, “Memory effect and bms-like symmetries for impulsive gravitational waves,” *Phys. Rev. D* **100** (Oct, 2019) 084010. <https://link.aps.org/doi/10.1103/PhysRevD.100.084010>.
- [39] S. Siddhant, I. Chakraborty, and S. Kar, “Kundt geometries and memory effects in the Brans-Dicke theory of gravity,” *Eur. Phys. J. C* **81** no. 4, (2021) 350.
- [40] S. Tahura, D. A. Nichols, A. Saffer, L. C. Stein, and K. Yagi, “Brans-dicke theory in bondi-sachs form: Asymptotically flat solutions, asymptotic symmetries, and gravitational-wave memory effects,” *Physical Review D* **103** no. 10, (May, 2021) . <https://dx.doi.org/10.1103/PhysRevD.103.104026>.
- [41] S. Tahura, D. A. Nichols, and K. Yagi, “Gravitational-wave memory effects in brans-dicke theory: Waveforms and effects in the post-newtonian approximation,” *Physical Review D* **104** no. 10, (Nov., 2021) . <https://dx.doi.org/10.1103/PhysRevD.104.104010>.
- [42] S. Bhattacharya, D. Bose, I. Chakraborty, A. Hait, and S. Mohanty, “Gravitational memory signal from neutrino self-interactions in supernova,” *Physical Review D* **110** no. 6, (Sept., 2024) . <https://dx.doi.org/10.1103/PhysRevD.110.L061501>.
- [43] I. Chakraborty, S. Bhattacharya, and S. Chakraborty, “Gravitational wave memory in wormhole spacetimes,” *Phys. Rev. D* **106** (Nov, 2022) 104057. <https://link.aps.org/doi/10.1103/PhysRevD.106.104057>.

- [44] S. Bhattacharya and S. Ghosh, “Gravitational wave memory for a class of static and spherically symmetric spacetimes,” 2023. <https://arxiv.org/abs/2309.04130>.
- [45] M. O’Loughlin and H. Demirchian, “Geodesic congruences, impulsive gravitational waves and gravitational memory,” *Phys. Rev. D* **99** no. 2, (2019) 024031, [arXiv:1808.04886](https://arxiv.org/abs/1808.04886) [hep-th].
- [46] M. S. Morris and K. S. Thorne, “Wormholes in space-time and their use for interstellar travel: A tool for teaching general relativity,” *Am. J. Phys.* **56** (1988) 395–412.
- [47] M. O’Loughlin and H. Demirchian, “Geodesic congruences, impulsive gravitational waves, and gravitational memory,” *Phys. Rev. D* **99** (Jan, 2019) 024031.
- [48] I. Chakraborty and S. Kar, “Geodesic congruences in exact plane wave spacetimes and the memory effect,” *Phys. Rev. D* **101** (Mar, 2020) 064022. <https://link.aps.org/doi/10.1103/PhysRevD.101.064022>.
- [49] R. M. Wald, *General Relativity*. Chicago Univ. Pr., Chicago, USA, 1984.
- [50] E. Poisson, *A Relativist’s Toolkit: The Mathematics of Black-Hole Mechanics*. Cambridge University Press, 12, 2009.
- [51] S. Kar and S. SenGupta, “The Raychaudhuri equations: A Brief review,” *Pramana* **69** (2007) 49, [arXiv:gr-qc/0611123](https://arxiv.org/abs/gr-qc/0611123).
- [52] S. Kar, “An introduction to the Raychaudhuri equations,” *Resonance J. Sci. Educ.* **13** (2008) 319–333.
- [53] J. Samuel, “Of Light and Shadows: Raychaudhuri’s Equation, the Big Bang and Black Holes,” *Reson.* **26** no. 1, (2021) 47–60, [arXiv:2012.14988](https://arxiv.org/abs/2012.14988) [physics.pop-ph].
- [54] T. Frankel, *Gravitational curvature*. W. H. Freeman, USA, 1979.
- [55] B. Carter, “Amalgamated Codazzi-Raychaudhuri identity for foliation,” *Contemp. Math.* **203** (1997) 207–219, [arXiv:hep-th/9705083](https://arxiv.org/abs/hep-th/9705083).
- [56] E. Zafiris, “Covariant generalization of Codazzi-Raychaudhuri and area change equations for relativistic branes,” *J. Geom. Phys.* **28** (1998) 271–288, [arXiv:hep-th/9710169](https://arxiv.org/abs/hep-th/9710169).
- [57] S. Ghosh, A. Dasgupta, and S. Kar, “Geodesic congruences in warped spacetimes,” *Phys. Rev. D* **83** (2011) 084001, [arXiv:1008.5008](https://arxiv.org/abs/1008.5008) [gr-qc].
- [58] P. Dutta Roy, S. Aneesh, and S. Kar, “Revisiting a family of wormholes: geometry, matter, scalar quasinormal modes and echoes,” *Eur. Phys. J. C* **80** no. 9, (2020) 850, [arXiv:1910.08746](https://arxiv.org/abs/1910.08746) [gr-qc].
- [59] V. Sharma and S. Ghosh, “Geodesic congruences in 5D warped Ellis–Bronnikov spacetimes,” *Eur. Phys. J. Plus* **137** no. 8, (2022) 881, [arXiv:2205.08865](https://arxiv.org/abs/2205.08865) [gr-qc].
- [60] E. Teo, “Rotating traversable wormholes,” *Phys. Rev. D* **58** (1998) 024014, [arXiv:gr-qc/9803098](https://arxiv.org/abs/gr-qc/9803098).
- [61] A. Kar, S. Jana, and S. Kar, “A new rotating lorentzian wormhole spacetime,” 2024. <https://arxiv.org/abs/2411.09202>.